Polymer Journal (2019) 51:449–459
https://doi.org/10.1038/s41428-018-0159-y

ORIGINAL ARTICLE

# Copolymerization of simple methacrylates by Cu(0)-mediated reversible deactivation radical polymerization

Jongwon Choe[1] · Woo Jung Lee[2] · Han Gyeol Jang[3] · Youngjoo Song[1] · Jae Hyun Sim[4] · Jaewoo Kim[3] · Keewook Paeng[2] · Myungwoong Kim[1]

Received: 10 August 2018 / Revised: 2 October 2018 / Accepted: 7 November 2018 / Published online: 13 December 2018


## Abstract

This study examined the kinetics of copolymerization of two different simple model monomers, methyl methacrylate (MMA), and ethyl methacrylate (EMA), via Cu(0)-mediated reversible deactivation radical polymerization (RDRP), where the reactivities of MMA and EMA are expected to be nearly equal, and therefore, random copolymerization is favored. In these kinetic studies, the apparent propagation rate constants and induction periods with variations in the feed ratio and polymerization temperature were estimated. The reactivity ratios determined based on the kinetic studies were close to unity. In addition, the reactivities of MMA and EMA radicals to both monomers were evaluated by determining the thermodynamic parameters of the activation processes; the reactions of active species with two different monomers experience slightly different enthalpic barriers but almost zero entropic contributions, strongly suggesting that the copolymerization provides an almost, but not perfectly, random sequence and providing a clear chemical picture of the propagation reaction that occurs during copolymerization. The glass transition studies of synthesized P(MMA-*r*-EMA) highlight the significance of the kinetic information to predict the glass transition temperature in a copolymer system realized by Cu(0)-mediated RDRP. The current study provides a deeper understanding of the fundamental aspects and a tool to gain insight into copolymerization via RDRP, which are ultimately correlated with various physical and chemical properties.

## Introduction

Reversible deactivation radical polymerization (RDRP), or controlled radical polymerization (CRP), has attracted tremendous attention as an excellent tool for the synthesis of well-defined polymers with narrow molecular weight distributions and precisely tailored functionalities [1–3]. RDRP enables the simultaneous achievement of a target molecular weight with narrow dispersity and a wide range of chemical functionalities in the resulting chain, as well as at the end of the chain, under relatively mild conditions [2]. These advantages have enabled the design and realization of complex polymer architectures, as well as the effective control of the physical, mechanical, and chemical properties of these polymers [3]. Owing to its capability, RDRP has become one of the essential polymerization methods to be expanded in fundamental soft matter research and used in a variety of applications [4].

Over the past decade, research on zero-valent metal-mediated RDRP (also called single-electron transfer living radical polymerization) has grown rapidly [5]. In polymerization, a zero-valent metal, typically Cu(0), is used as a catalyst precursor that is activated in the presence of an

**Electronic supplementary material** The online version of this article (https://doi.org/10.1038/s41428-018-0159-y) contains supplementary material, which is available to authorized users.

✉ Keewook Paeng
paeng@skku.edu

✉ Myungwoong Kim
mkim233@inha.ac.kr

[1] Department of Chemistry and Chemical Engineering, Inha University, Incheon 22212, Republic of Korea

[2] Department of Chemistry, Sungkyunkwan University, Suwon 16419, Republic of Korea

[3] Institute of Advanced Composite Materials, Korea Institute of Science and Technology (KIST), Jeollabuk-do 55324, Republic of Korea

[4] Department of Chemistry, Hanyang University, Seoul 04763, Republic of Korea

amine ligand. The characteristics of Cu(0)-mediated RDRP are similar to those of atom transfer radical polymerization (ATRP) in terms of simultaneous use of copper species and an amine ligand; however, in Cu(0)-mediated RDRP, Cu(0) is generated continuously from Cu(I) complexes by disproportionation, and this Cu(0) acts as a catalyst for radical generation in the polymerization system [5]. This process offers different benefits from other RDRP techniques; for example, the chain end can include a much wider range of chemical functionality, such as carbon halides (in the case of an initiator for ATRP) [6] and thioesters (in the case of a reversible addition fragmentation chain transfer (RAFT) polymerization chain transfer agent as an initiator) [7], which should be beneficial for achieving complex polymer architectures. Cu(0)-mediated RDRP is a versatile technique that allows the rapid polymerization of styrene, acrylamides, acrylates, and methacrylates in polar solvents, such as dimethyl sulfoxide (DMSO), dimethyl formamide (DMF), and water, even at room temperature [8, 9]. In addition, Cu(0)-mediated RDRP can be used to synthesize high-molecular-weight polymers (even higher than $5 \times 10^5$ g/mol) with well-controlled dispersity (<1.3) and preserved functionalities, which could not be achieved by conventional free radical polymerizations [1, 9]. For these reasons, Cu(0)-mediated RDRP has attracted attention as a promising polymerization method to generate advanced soft materials in a number of research fields.

Copolymerization is an important and powerful method to impart and control a range of properties in polymers. In RDRP, copolymerization has been used extensively for a number of applications [10–16], e.g., control of microphase separation to create periodic nanopatterns [17–22], fabrication of functional stable thin films [23–26], and stabilization of colloidal micelles and particles [27–31]. Despite the significance of copolymerization, fundamental aspects of copolymerization, such as reactivity ratios to gain insight into the copolymer sequence, have not been thoroughly investigated. As a result, we often rely on kinetic studies mainly of conventional free radical polymerization [32–36] with some observation that radical processes intrinsically exhibit the same or similar reactivity between active species and monomers [37]. In RDRP, copolymerization kinetics of common monomer pairs used in ATRP and RAFT polymerization have been reported [2, 38–41]. In the case of Cu (0)-mediated RDRP, there are a few reports describing detailed kinetics and reactivity ratios [42]. Systematic studies on the fundamentals, such as the copolymerization kinetics of simple monomer pairs to exclude the effects of other structural factors, are necessary to compare kinetic information of RDRP, for example, the reactivity ratios, with that of other conventional polymerization processes. Furthermore, activation during the propagation process of RDRP, i.e., thermodynamically described enthalpic and entropic contributions during activation, should be studied thoroughly to better understand the copolymerization processes. Accordingly, a comparison of various kinetic and thermodynamic parameters of RDRP to those of other radical polymerization processes will reinforce the fundamental principles and provide other important information, such as the sequence and structure of a synthesized copolymer. Ultimately, such studies will provide fundamental perspectives and tools to gain insight into the effects of the sequence of well-defined copolymers with precisely controlled functionalities on a variety of properties.

Herein, we performed thorough kinetic studies of the copolymerization of two simple model monomers, methyl methacrylate (MMA) and ethyl methacrylate (EMA), which are widely used as comonomers to realize functional soft material platforms [43–45], via Cu(0)-mediated RDRP. MMA, and EMA are the simplest methacrylates with minimal structural variation and without any reactive groups. In principle, copolymerization of the monomers preferentially results in *statistical* copolymers following zeroth-order Markovian statistics (also called Bernoullian statistics) or *random* copolymers [46], as the reactivity is expected to be similar to each other. Ideally, it is possible to determine the intrinsic reactivity of the alkene moiety of methacrylates by radical propagation in Cu(0)-mediated RDRP, which can be examined by excluding the effects of other structural parameters in careful and thorough copolymerization kinetic studies. The results will provide us with chemical and physical insight into the polymerization process, e.g., the randomness of the synthesized copolymers, its significance in predicting the thermal properties of the copolymers and achieving a complex polymer chain structure containing a random sequence along the chain.

In Cu(0)-mediated RDRP using a RAFT chain transfer agent as an initiator, we examined the kinetics of copolymerization as a function of the monomer feed and polymerization temperature. We found that the experimental data followed typical pseudo-first-order reaction kinetics. With these studies, the reactivity ratios of MMA and EMA were estimated at different temperatures and compared with those of other polymerization methods. The results strongly suggest that the resulting copolymers have random sequences at low conversion (~10%). Further analyses of the reactivity ratio and compositional studies of copolymers synthesized at high conversion (~60%) allow determination of the thermodynamic parameters, i.e., enthalpic barriers and entropic contributions in propagation reactions of different intermediate species and monomeric species, and their effect on copolymer sequences, providing a clear kinetic and thermodynamic picture of the propagation reaction as well as the randomness of the sequence. The glass transition behaviors of the synthesized copolymers, which are expected to deviate systematically from those of

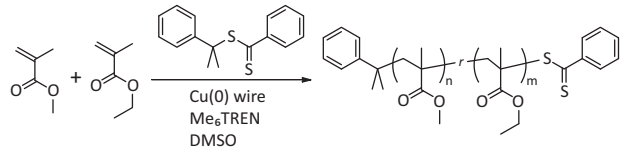


**Scheme 1** Synthesis of P(MMA-*r*-EMA) by Cu(0)-mediated RDRP

PMMA and PEMA homopolymers, were examined further [47]. The empirical model that is most appropriate for predicting the change in the glass transition temperature ($T_g$) of P(MMA-*r*-EMA) was analyzed as a function of the composition, highlighting the importance of the reactivity ratio in determining the model to predict $T_g$. Finally, the ability of the random copolymer to serve as a macro chain transfer agent for RAFT polymerization was evaluated in the synthesis of P(MMA-*r*-EMA)-*b*-polystyrene, which is essential for achieving complex copolymer systems.

## Experimental section

### Copolymerization of MMA and EMA via Cu(0)-mediated RDRP

Eighteen pieces of Cu(0) wire were placed in a Schlenk flask equipped with a stirring bar. Predetermined amounts of MMA and EMA (total = 18.8 mmol) at various feed ratios were added to the flask. Subsequently, tris(2-dimethylaminoethyl)amine ($Me_6$TREN, 9.4 µmol, 2.2 mg), cumyl dithiobenzoate (CDB, 9.4 µmol, 2.6 mg) and DMSO (0.88 mL) were added to the flask with a stock solution of $Me_6$TREN and CDB in DMSO. The mixture was degassed by three freeze-pump-thaw cycles, followed by placing the flask in a preheated oil bath to begin polymerization. After the desired polymerization time, an aliquot of the solution was taken to determine the level of conversion using $^1$H nuclear magnetic resonance (NMR) spectroscopy (Figure S2). In the case of a highly viscous solution, a small amount of chloroform (1-2 ml) was added to the mixture to enable removal of an aliquot. The remaining mixture in the flask was diluted with tetrahydrofuran (THF) and passed through a neutral alumina column to remove the copper residue. The polymer solution was added to methanol for precipitation, resulting in a pale pink powder. The product was dried further under vacuum for 10 h.

### Chain extension of P(MMA-*r*-EMA) with styrene

First, 1 µmol of P(MMA-*r*-EMA) (22–32 mg depending on $M_n$) and azobisbutyronitrile (AIBN, 0.45 µmol) were dissolved in styrene (1.35 mmol, 141 mg) in a Schlenk flask. A 2.9 mM solution of AIBN in styrene was used as the stock solution. The mixture was degassed by three freeze-pump-thaw cycles and placed in a preheated oil bath at 70 °C for 15 h with stirring. After polymerization, the contents were diluted with THF, followed by precipitation in *n*-hexane to yield a pale pink powder. The product was dried under vacuum for more than 10 h.

### Characterization

The $^1$H-NMR spectra were acquired on a JEOL JNM-ECZ400S 400 MHz spectrometer using chloroform-*d* (Cambridge isotope) as a solvent to analyze the conversion and polymer composition. The chloroform peak at 7.26 ppm was used as an internal reference. All measurements were carried out with 10 s relaxation delays between pulses. Size-exclusion chromatography (SEC) was performed on a Thermo Scientific UltiMate 3000 chromatography system using THF as the eluent at a flow rate of 1 mL/min at 35 °C. Three SEC columns (Styragel HR5, Styragel HR4, and Styragel HR3, Waters, calibrated using polystyrene (PS) standard samples of 1.2–2700 kg/mol) were used in the system. Differential scanning calorimetry (DSC) was performed with a 10 K/min ramping rate for three cycles. The glass transition temperature was determined from the inflection point of the DSC curve from the third cooling cycle. More details on the experiments and analyses are provided in the Supplementary Information.

## Results and discussion

### Copolymerization kinetics

Scheme 1 presents the copolymerization of MMA and EMA via Cu(0)-mediated RDRP using a RAFT agent as an initiator [1]. In particular, we designed experiments to explore the effects of various copolymerization conditions, i.e., feed ratio ($f_{EMA}$ ~ 0.2, 0.5, 0.8), temperature (~60 °C, 80 °C, and 100 °C), and polymerization time, with $[Monomer]_0/[CDB]_0/[Me_6TREN]_0 = 2000:1:1$ in DMSO. In this polymerization system, Cu(0), $Me_6$TREN, and CDB were used as catalyst precursors, which are a primarily activated species, an amine-containing ligand, and a chain transfer agent, respectively [1]. Cu(0) activates the radicals for initiation in the presence of the ligand, $Me_6$TREN, leading to the formation of a Cu(I)-ligand complex. Under these conditions, the polymerization solution typically becomes highly viscous when the conversion reaches more than 60%. Figure 1 shows the kinetic plots as a function of the polymerization time and conversion at various temperatures and feed ratios. The propagation rate in a CRP typically follows a first-order reaction at a moderate conversion regime (<50%), indicating that polymerization is barely

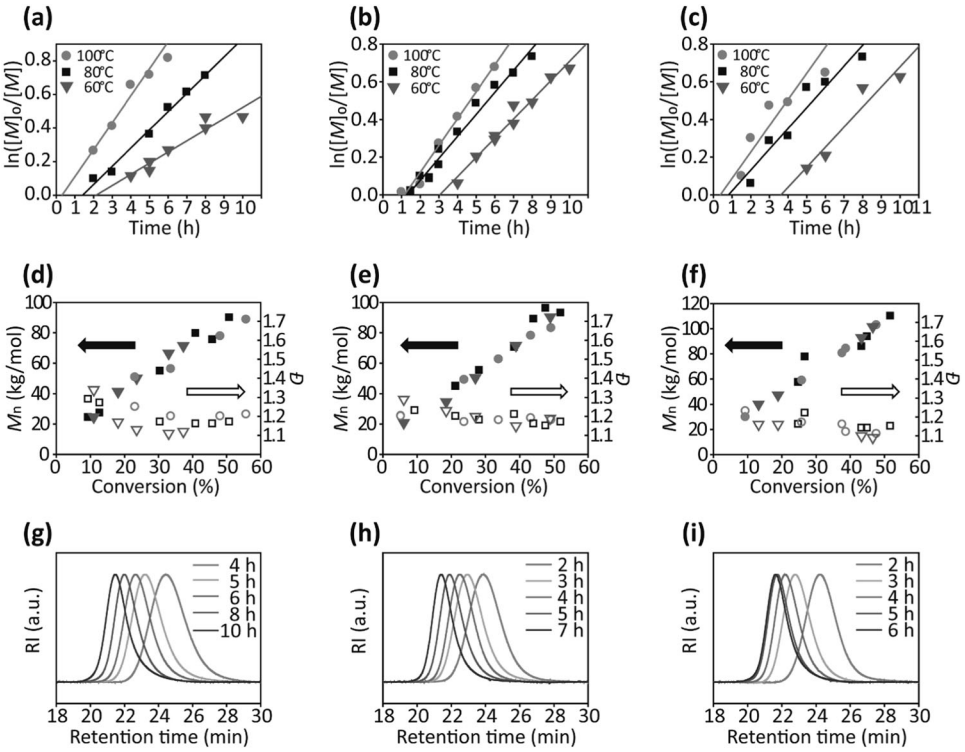


**Fig. 1** **a–c** Linear fit for a kinetic study at 100 °C (red circles), 80 °C (black squares) and 60 °C (blue triangles) with various EMA feed ratios: **a** $f_{EMA} = 0.2$, **b** $f_{EMA} = 0.5$, **c** $f_{EMA} = 0.8$. **d–f** Number average molecular weight ($M_n$) and dispersity ($Đ$) depending on the conversion for each EMA ratio: **d** $f_{EMA} = 0.2$, **e** $f_{EMA} = 0.5$, **f** $f_{EMA} = 0.8$. **g–i** The SEC trace for $f_{EMA} = 0.5$ at (**g**) 60 °C, (**h**) 80 °C and (**i**) 100 °C

**Table 1** Estimated apparent propagation rate constants and induction periods at different temperatures and monomer feed ratios

| $f_{EMA}$ | Temperature (°C) | $k_p^{app}$ ($h^{-1}$) | $t_{id}$ (h) |
|---|---|---|---|
| 0.2 | 60 | 0.067 ± 0.009 | 2.1 |
| | 80 | 0.109 ± 0.006 | 1.4 |
| | 100 | 0.161 ± 0.024 | 0.3 |
| 0.5 | 60 | 0.102 ± 0.007 | 3.0 |
| | 80 | 0.117 ± 0.006 | 1.3 |
| | 100 | 0.143 ± 0.009 | 1.1 |
| 0.8 | 60 | 0.106 ± 0.023 | 3.7 |
| | 80 | 0.110 ± 0.016 | 0.8 |
| | 100 | 0.139 ± 0.051 | 0.3 |

influenced by the increased viscosity and termination reactions [48]. The rate of propagation typically follows Eq. (1):

$$R_p = k_p[M^*][M] = k_p^{app}[M] \quad (1)$$

where $R_p$ is the rate of propagation and $k_p$ is a rate constant of the propagation reaction. When a steady-state approximation is assumed, i.e., the concentration of active radical species ($[M^*]$) is a constant and all active radical species have the same chance to exist in Cu(0)-mediated RDRP, the rate of propagation should follow a first-order reaction with an apparent kinetic constant of $k_p^{app}$, the so-called pseudo-first-order reaction. In the rate law, the concentration of monomer ($[M]$) can be correlated with the polymerization time, resulting in Eq. (2), as follows:

$$\ln\left([M]_0/[M]\right) = k_p^{app}t \quad (2)$$

where $[M]_0$ is the initial concentration of the monomer. Therefore, the rate constant of propagation is evaluated by examining a plot of $\ln([M]_0/[M])$ vs. polymerization time. Figure 1a–c shows nine different plots with systematic variation in the feed ratio and reaction temperature. The $k_p^{app}$ values were extracted from the slopes of the straight lines produced by a linear fit of the plots and are tabulated in Table 1.

The results show a nonsignificant difference in the apparent kinetic constant with variation in the feed ratio at the same reaction temperature. This suggests that the reactivity of EMA is similar to the reactivity of MMA, which is expected for the monomer pair. The rate constant tended to increase as the temperature increased from 60 to 100 °C, regardless of the changes in the feed ratio, which can be predicted using the Arrhenius relationship. It should be noted that in the initiation process, an induction period ($t_{id}$) of a few hours was observed. Furthermore, the induction period decreased with increasing temperature; this behavior could be attributed to the use of dithioesters (CDB) [49, 50]. In the initiation stage, the dithioester compound is not as reactive for propagation because no adduct radicals have yet been generated. The propagation begins once monomer is added to CDB and equilibrium is achieved. When the

temperature increases, the fragmentation of CDB to reach equilibrium becomes faster; as a consequence, the induction period decreased significantly. Additionally, the role of the heterogeneous Cu(0) wires could not be underestimated. The radical-activation process with copper atoms on the wire surface is slow in the initial stages due to the low surface area. Once the Cu(I) complex forms, Cu(0) is regenerated continuously from the Cu(I) complex by a disproportionation mechanism in the presence of a ligand and polar solvent. The Cu(0) particles are well distributed in the reaction medium, and the propagation process can proceed efficiently. When the temperature was increased from 60 °C to 100 °C, the formation of a Cu(I) complex became faster, resulting in a decrease in the induction period.

Figure 1d–f displays $M_n$ (left *y*-axis) and dispersity (right *y*-axis) as a function of conversion. Regardless of the reaction temperature and feed ratio, the degree of polymerization clearly exhibited a linear increase as the conversion increased, which is a typical characteristic of RDRP [3]. Fig. 1g–i and Figure S1 present all of the corresponding SEC chromatograms for the data points; all peaks were unimodal and clearly upshifted to a higher molecular weight range as polymerization proceeded. The dispersity decreased from ~1.3 to <1.2 (even <1.1) as the conversion increased, indicating that polymerization is highly controlled. We observed that the kinetic parameters did not follow the pseudo-first-order reaction at conversions higher than 60% due to the viscosity effect.

## Determination and interpretation of reactivity ratios

A variety of monomers exhibit different reactivities with activated radical species and therefore different propagation rates. During copolymerization, different monomers in the same polymerization reaction also exhibit different reactivities toward radicals at the end of the polymer chain. Consequently, the composition of the resulting polymer chain is often not equal to the amount fed for polymerization. This behavior is quantified using the reactivity ratios, namely, $r_1$ and $r_2$ (herein, $r_{EMA}$ and $r_{MMA}$), which describe the distribution of fed monomers in a synthesized single-copolymer chain, as found in the Mayo-Lewis equation [51]:

$$F_1 = \frac{(r_1 - 1)f_1^2 + f_1}{(r_1 + r_2 - 2)f_1^2 + 2(1 - r_2)f_1 + r_2} \quad (3)$$

where $f_1$ is the mole fraction of monomer 1 in the feed and $F_1$ is the mole fraction of monomer 1 in the actual composition of the resulting copolymer. Since the equation is derived under the assumption that the radical concentration is at a steady state, where the effect of any other factors, such as termination and viscosity effect on propagation is minimized, the actual composition of the synthesized copolymers ($F_{EMA}$) was measured according to the variation in $f_{EMA}$ at conversion in the range of 5–15%. As the propagation rate varies with different reaction conditions and feed ratios, the reaction conditions were controlled carefully based on kinetic studies of copolymerization. Appropriate conversions in the given range were typically achieved with polymerization for 4, 2, and 1.5 h at 60 °C, 80 °C, and 100 °C, respectively. The conversion and composition of the resulting copolymer samples were analyzed by $^1$H-NMR spectroscopy. As shown in Figure S2, protons of $CH_3$–O– in the MMA monomer and –$CH_2$–O– in the EMA monomer appeared at 3.7 ppm and 4.2 ppm, respectively. Upon polymerization, the peaks were shifted slightly upfield, allowing an estimation of the conversion and composition by integrating the characteristic peaks of the monomers and the polymer. The plots constructed from the compositional data were analyzed using three different methods: nonlinear least-squares fitting with the Mayo-Lewis equation, the Fineman-Ross method, and the Kelen-Tudos method (see Supplementary Information for details) [52–54].

Figure 2a–c shows plots of the actual composition as a function of the monomer feed ratio at 60, 80, and 100 °C. At first glance, the composition of the synthesized copolymers is very close to the feed amount of the monomers regardless of the temperature. The red solid lines in Fig. 2a–c represents the results obtained by nonlinear least-squares fitting with the Mayo-Lewis equation, and Table 2 lists the $r_{EMA}$ and $r_{MMA}$ values extracted from the fits. Figure S3 shows a linear fit of copolymers obtained at 80 °C using the Fineman-Ross (Figure S3a) and Kelen-Tudos (Figure S3b) models. All calculated reactivity ratio values fell within the range of 0.91–1.02. Considering the empirical errors given in the table, both $r_{EMA}$ and $r_{MMA}$ are close to 1, indicating that the reactivities of MMA and EMA toward the activated MMA radical or EMA radical at the chain end are nearly identical. In other words, the relative rate constants of the two monomers in chain extension are similar regardless of the end unit of the polymer chains during propagation. This similarity is found in the literature reporting bulk free radical copolymerization at 60 °C: $r_{EMA}$ and $r_{MMA}$ were found to be $0.98 \pm 0.1$ and $1.09 \pm 0.1$, respectively [55]. This was also observed by analyzing the composition data using the Fineman-Ross and Kelen-Tudos methods; $r_{EMA}$ and $r_{MMA}$ were in the range of 0.90–1.08 and 0.89–1.05, respectively.

To illustrate the effects of the reactivity ratio of each monomer on the sequence of copolymer chains, the fractions of the dyad monomer sequences, i.e., EMA-EMA, MMA-MMA, and EMA-MMA, were calculated as a function of $F_{EMA}$ with the Igarashi method using equations

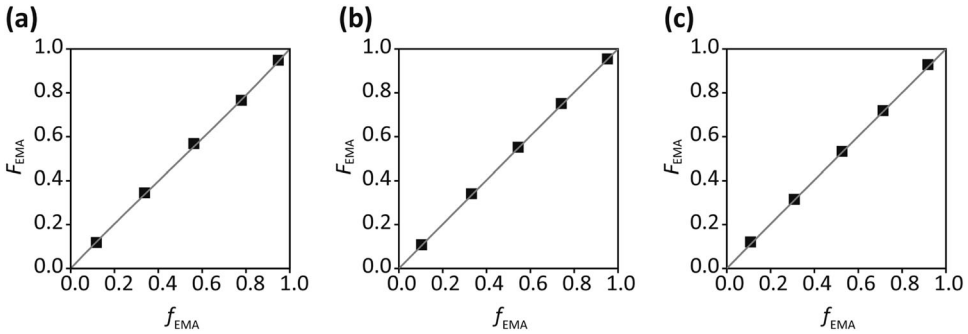


**Fig. 2** Plots of the composition of EMA ($F_{EMA}$) vs. EMA feed ratio ($f_{EMA}$) to calculate the reactivity ratios by nonlinear least-squares fitting with the Mayo-Lewis equation at **a** 60 °C, **b** 80 °C and **c** 100 °C

**Table 2** Reactivity ratios for P(MMA-*r*-EMA) obtained using different models

| Temperature | Method | $r_{EMA}$ | $r_{MMA}$ |
|---|---|---|---|
| 60 °C | NLS fit[a] | 0.91 ± 0.05 | 0.95 ± 0.05 |
| | FR[b] | 0.90 ± 0.01 | 0.98 ± 0.06 |
| | KT[c] | 0.90 ± 0.06 | 0.98 ± 0.05 |
| 80 °C | NLS fit | 1.02 ± 0.02 | 0.99 ± 0.02 |
| | FR | 0.93 ± 0.01 | 0.89 ± 0.07 |
| | KT | 0.96 ± 0.05 | 0.97 ± 0.04 |
| 100 °C | NLS fit | 1.00 ± 0.03 | 0.98 ± 0.03 |
| | FR | 1.08 ± 0.01 | 1.05 ± 0.06 |
| | KT | 1.03 ± 0.07 | 0.97 ± 0.04 |

Obtained with [a]nonlinear least-squares fitting with the Mayo-Lewis equation

[b]Fineman-Ross method

[c]Kelen-Tudos method

(S5)–(S7) (Figure S4). The dyad fraction is dependent on the product of $r_{EMA}$ and $r_{MMA}$; therefore, we used minimum and maximum $r_{EMA}r_{MMA}$ values (0.83 and 1.13, respectively) to show the possible ranges of the dyad fractions. The studies clearly show that the reactivities of both monomers are comparable during copolymerization. Additionally, in Cu(0)-mediated RDRP, copolymerization of the two simple methacrylate monomers leads to a composition close to a random sequence distribution in the resulting copolymer chains. These results strongly suggest that the intrinsic reactivities of these two simple methacrylates are almost identical, even with different active chain end species, thereby substantiating the common assumption that the reactivity ratio is universally valid in radical-based polymerization.

Since the reactivity ratios of the monomers are defined as the ratios of the rate constants, they are expected to be temperature dependent. In this system, the temperature dependence of the reactivity ratios was observed; $r_{EMA}$ increased slightly with increasing polymerization temperature, but $r_{MMA}$ showed less temperature dependence. This dependence can be interpreted thermodynamically using an equation derived from the Arrhenius equation, as given below [56]:

$$r_{EMA} = e^{\frac{\Delta S^{\ddagger}_{EMA-EMA} - \Delta S^{\ddagger}_{EMA-MMA}}{R} - \frac{\Delta H^{\ddagger}_{EMA-EMA} - \Delta H^{\ddagger}_{EMA-MMA}}{RT}} \quad (4)$$

where $\Delta S^{\ddagger}_{EMA\text{-}EMA} - \Delta S^{\ddagger}_{EMA\text{-}MMA}$ and $\Delta H^{\ddagger}_{EMA\text{-}EMA} - \Delta H^{\ddagger}_{EMA\text{-}MMA}$ are the activation entropy and activation enthalpy differences for the propagation of the EMA radical at the chain end with the EMA monomer and for the propagation of the EMA radical at the chain end with the MMA monomer, respectively. In addition, $r_{MMA}$ is related to $\Delta S^{\ddagger}_{MMA\text{-}MMA} - \Delta S^{\ddagger}_{MMA\text{-}EMA}$ and $\Delta H^{\ddagger}_{MMA\text{-}MMA} - \Delta H^{\ddagger}_{MMA\text{-}EMA}$ in the same manner. With the experimental data set, a plot of ln *r* vs. 1/T enables calculation of the entropy and enthalpy differences between the reaction of an active radical with the same species and different species. Figure 3 displays plots of ln $r_{EMA}$ and ln $r_{MMA}$ as a function of the reciprocal temperature, and linear fits were obtained from the reactivity ratio data using three different methods. The entropy and enthalpy differences for $r_{EMA}$ and $r_{MMA}$ were also calculated, as shown in Table 3. The difference in activation entropy for both cases approached zero, indicating that the steric effect on the reaction is not significant for the reaction of the MMA or EMA chain end radicals with either monomer. On the other hand, the activation enthalpy differences for both were quite dissimilar; $\Delta H^{\ddagger}_{EMA\text{-}EMA} - \Delta H^{\ddagger}_{EMA\text{-}MMA}$ was approximately three times higher than $\Delta H^{\ddagger}_{MMA\text{-}MMA} - \Delta H^{\ddagger}_{MMA\text{-}EMA}$. This finding suggests that more energy is needed for the EMA radical with MMA than for the MMA radical with EMA. Nevertheless, the absolute values are actually very small (approaching zero) for both cases compared to the literature values for other monomer pairs exhibiting quite different reactivities [56–58]. This strongly suggests that the copolymerization of MMA and EMA results in a sequence that has a nearly, but not perfectly, random composition.

We further conducted compositional studies at conversion much higher than 60%, where high-molecular-weight copolymers can be achieved. Table 4 lists the characterization results of the copolymers. At ~60% conversion, high-molecular-weight copolymers with very low dispersity of as low as 1.08 were synthesized,

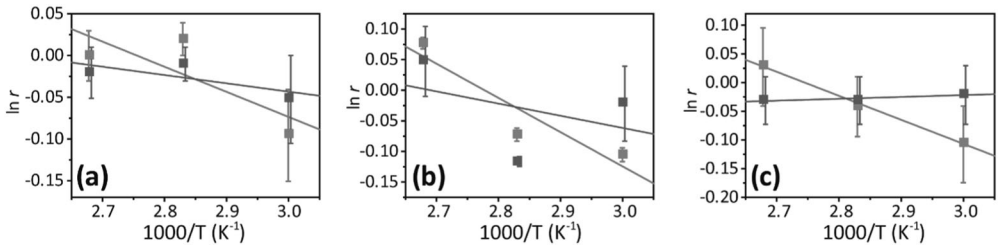


**Fig. 3** Plots of the natural logarithm of $r_{EMA}$ (red trace) and $r_{MMA}$ (blue trace) obtained by **a** nonlinear fitting, **b** the Fineman-Ross method, and **c** the Kelen-Tudos method as a function of reciprocal temperature

**Table 3** Thermodynamic information about the propagation reactions

| $M_1/M_2$ | Method | $\Delta H^{\ddagger}_{11}$ - $\Delta H^{\ddagger}_{12}$ ($J \cdot mol^{-1}$) | $\Delta S^{\ddagger}_{11}$ - $\Delta S^{\ddagger}_{12}$ ($J \cdot mol^{-1} \cdot K^{-1}$) |
|---|---|---|---|
| EMA/MMA | NLS fit | 36.2 ± 27.7 | 0.10 ± 0.079 |
| | FR | 67.3 ± 27.4 | 0.19 ± 0.078 |
| | KT | 50.3 ± 2.9 | 0.14 ± 0.008 |
| MMA/EMA | NLS fit | 12.0 ± 10.7 | 0.03 ± 0.030 |
| | FR | 23.9 ± 57.3 | 0.06 ± 0.163 |
| | KT | −3.9 ± 2.1 | −0.01 ± 0.006 |

regardless of the variation in $f_{EMA}$. This result confirms that Cu(0)-mediated RDRP is beneficial for the copolymerization of methacrylates over a wide range of conversion. The resulting $F_{EMA}$ from $f_{EMA}$ is typically less than 0.05; interestingly, the variation showed fewer EMA units for all compositions. These results further support the observation of enthalpic barriers discussed in the previous section; slightly more energy was necessary for EMA radicals to react with EMA than to react with MMA. As the conversion increased, the amount of MMA units in the copolymer chain increased slightly above that of EMA. Therefore, these results highlight the importance of a close examination of the copolymerization kinetics for a deeper understanding of the copolymer structure at both high and low conversion.

## Glass transition behaviors of the random copolymers

The glass transition behaviors of P(MMA-*r*-EMA) copolymers synthesized by Cu(0)-mediated RDRP were studied by measuring the $T_g$ of a series of copolymers and homopolymers with high-molecular weights (Table 4). The $M_n$ of polymers with molecular weights higher than ~100 kg/mol were attained to exclude the effects of the molecular weight on $T_g$. Figure 4a shows the change in $T_g$ according to the composition. The compositional dependence of $T_g$ has been interpreted using a number of models; the simplest models are the Fox equation, Eq. (5), and the Gibbs-DiMarzio (GD)

**Table 4** Composition, molecular weight, and glass transition temperature of PMMA, PEMA, and P(MMA-*r*-EMA) synthesized at high conversion

| $f_{EMA}$ | $F_{EMA}$ | $M_n$ (kg/mol) | $Đ$ | $T_g$ (K)[a] |
|---|---|---|---|---|
| 0 | 0 | 126.7 | 1.11 | 393 |
| 0.40 | 0.37 | 99.2 | 1.10 | 368 |
| 0.55 | 0.48 | 161.5 | 1.10 | 363 |
| 0.69 | 0.63 | 145.4 | 1.15 | 357 |
| 0.85 | 0.80 | 139.4 | 1.08 | 350 |
| 1 | 1 | 163.5 | 1.09 | 346 |

[a]Determined by finding the point of inflection in the DSC curve acquired at the third cooling cycle with a ramping rate of 10 K/min

equation, Eq. (6) [59, 60]:

$$\frac{1}{T_g} = \frac{w_1}{T_{g1}} + \frac{w_2}{T_{g2}} \tag{5}$$

$$T_g = n_1 T_{g1} + n_2 T_{g2} \tag{6}$$

where $w_x$ and $n_x$ are the weight fraction and mole fraction of monomer unit $x$, respectively, in the copolymer chain, and $T_{gx}$ is the $T_g$ of homopolymer consisting of monomer unit $x$ ($x = 1$: EMA; $x = 2$: MMA). The compositional dependence of the $T_g$ of P(MMA-*r*-EMA) did not follow either model, as shown in Fig. 4a.

Therefore, we attempted to use other more complicated models that take monomer sequence information (see Supplementary Information and the dyad fractions shown in Figure S4) into account, i.e., the Johnston equation and the Barton equation given by Eqs. (7) and (8), respectively [61, 62]:

$$\frac{1}{T_g} = \frac{w_1 P_{11}}{T_{g11}} + \frac{w_2 P_{22}}{T_{g22}} + \frac{w_1 P_{12} + w_2 P_{21}}{T_{g12}} \tag{7}$$

$$T_g = n_{11} T_{g11} + n_{22} T_{g22} + n_{12} T_{g12} + n_{21} T_{g21} \tag{8}$$

where $T_{g12}$ (also equal to $T_{g21}$) is the $T_g$ of an alternating copolymer consisting of monomers 1 and 2. Since it is difficult to realize a perfect alternating copolymer, this

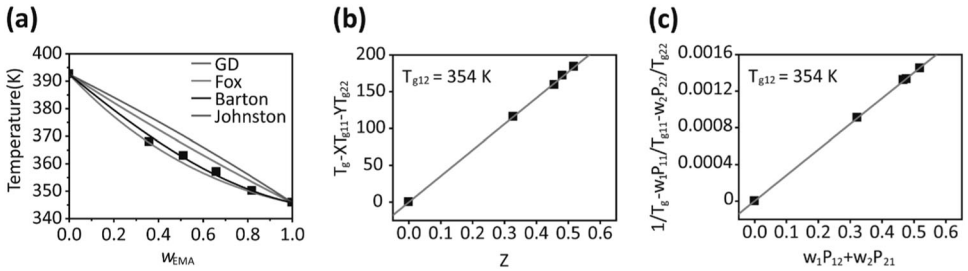


**Fig. 4** **a** Composition dependence of $T_g$ of the synthesized P(MMA-*r*-EMA) samples and fitting results from four different methods. The fitting results obtained using the Barton and Johnston equations are shown in (**b**) and (**c**)

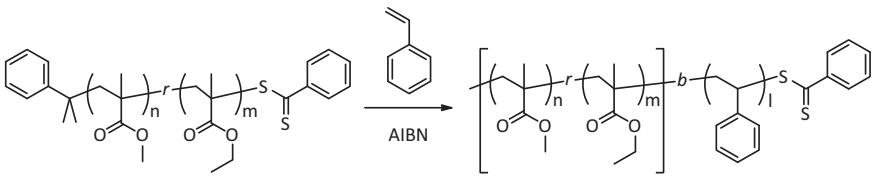


**Scheme 2** Chain extension of P(MMA-*r*-EMA) with styrene by RAFT polymerization

**Table 5** Characterization results of the synthesized P(MMA-*r*-EMA) and P(MMA-*r*-EMA)-*b*-PS

| P(MMA-*r*-EMA) | | | | P(MMA-*r*-EMA)-*b*-PS | | | | |
|---|---|---|---|---|---|---|---|---|
| $F_{EMA}$[b] | $M_n$ (kg/mol)[a] | $Đ$[a] | $T_g$ (K)[c] | $M_n$ (kg/mol)[a] | $Đ$[a] | $M_n$(PS) (kg/mol)[a] | MMA:EMA:Styrene[b] | $T_g$ (K)[c] |
| 0.12 | 23.7 | 1.27 | 377.8 | 35.9 | 1.32 | 12.2 | 0.63:0.09:0.28 | 381 |
| 0.34 | 28.1 | 1.21 | 365.3 | 45.1 | 1.38 | 17.0 | 0.36:0.18:0.46 | 375 |
| 0.57 | 35.0 | 1.22 | 361.2 | 62.0 | 1.34 | 27.0 | 0.20:0.29:0.51 | 372 |
| 0.95 | 36.1 | 1.18 | 346.5 | 42.0 | 1.23 | 5.9 | 0.05:0.80:0.15 | 350 |

[a]Measured with SEC analysis with THF as the eluent and calibration with PS standard samples

[b]Obtained from $^1$H-NMR spectra

[c]Determined by finding the point of inflection in the DSC curve acquired during the third cooling cycle with a ramping rate of 10 K/min

quantity is typically obtained by fitting. In the case of the Johnston model, the fitting of the data with Eq. (7) enabled determination of $T_{g12}$, and in the case of the Barton model, the value can be calculated by fitting with Eq. (9):

$$T_g = XT_{g11} + YT_{g22} + ZT_{g12} \quad (9)$$

To carry out this analysis, we used the dyad fractions (X, Y, Z), which were calculated using the reactivity ratios ($r_{EMA} = 0.91$, $r_{MMA} = 0.95$) from the experimental data acquired at 60 °C for the series of synthesized copolymers. The $T_{g12}$ values determined by the Johnston and Barton models were both 354 K. The compositional dependence of $T_g$ of P(MMA-*r*-EMA) copolymers synthesized by bulk radical polymerization has been well described using the Barton equation with a $T_{g12}$ of 360 K [47], which is in good agreement with our results. Therefore, the compositional dependence of $T_g$ follows these models rather than the Fox and GD models, emphasizing that the kinetic parameters should not be overlooked when predicting the glass transition behaviors of random copolymers synthesized by Cu(0)-mediated RDRP.

## Chain extension from the copolymer with styrene

Since the dithioester group in the resulting random copolymers is expected to be preserved upon Cu(0)-mediated RDRP, chain extension should be possible by RAFT polymerization [1]. This process also allows access to the block copolymer consisting of a random copolymer block and a homopolymer block. For proof of concept, P(MMA-*r*-EMA)-*b*-PS block copolymers were synthesized via RAFT polymerization of styrene, with P(MMA-*r*-EMA) as a macro chain transfer agent and AIBN as an initiator (Scheme 2). The copolymers were synthesized at low conversion to ensure that the copolymers indeed had an almost random sequence. As shown in Table 5 and Fig. 5a–d, the chain extensions were successful; increases in molecular weight without any significant increases in dispersity were observed. Note that all BCPs show unimodal SEC traces, indicating that no undesired polymers were produced in the course of the chain extension. The synthesized BCPs were further characterized by DSC. In particular, the glass transition temperature was measured to determine the effects of the copolymer structure on the thermal properties. Figure 5e, f displays the DSC curves of

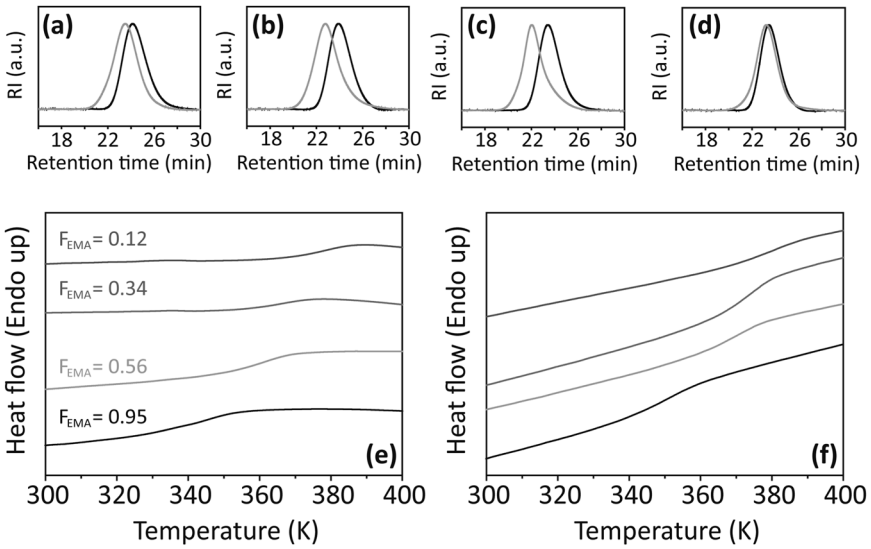


**Fig. 5** SEC chromatograms of P(MMA-*r*-EMA) (black trace) with **a** $F_{EMA} = 0.12$, **b** $F_{EMA} = 0.34$, **c** $F_{EMA} = 0.56$, **d** $F_{EMA} = 0.95$, and P(MMA-*r*-EMA)-*b*-PS grown from corresponding random copolymers (red trace), and DSC curves of (**e**) random copolymers and (**f**) of the BCPs extended with styrene

four P(MMA-*r*-EMA)s and the BCPs upon chain extension of the copolymers. The BCPs exhibit only one $T_g$ value rather than two $T_g$ values. One $T_g$ value was expected for the BCPs because the $T_g$ values of P(MMA-*r*-EMA) are similar to the $T_g$ of PS (354–368 K, estimated from measured $M_n$(PS) using the empirical equation $T_g = 371 - (10^5/M_n)$)[63]. These results also confirm the successful chain extension of P(MMA-*r*-EMA), highlighting the ability to achieve complex copolymers with well-controlled structures.

## Conclusions

The copolymerization of two simple methacrylates, MMA and EMA, via Cu(0)-mediated RDRP was thoroughly studied. Cu(0)-mediated RDRP offers a highly controlled route to form copolymers exhibiting desired molecular weights, low dispersity, and end functionality. Kinetic studies with systematic variations in the monomer feed ratio and temperature showed that the copolymerization followed pseudo-first-order reaction kinetics; the apparent rate constant did not show a significant difference regardless of the monomer feed ratio, although the polymerization temperature affected the rate constant and induction period. In addition, the degree of polymerization of all copolymers increased linearly as a function of polymerization conversion. The reactivity ratios as a function of temperature were obtained using three different methods. The reactivity ratios of MMA and EMA were close to unity, indicating that the copolymer has a nearly random sequence. The temperature dependence of the reactivity ratios provided thermodynamic information, i.e., enthalpic barriers and entropic contributions in the propagation reactions of the same monomer species or different monomer species. The difference in activation entropy for both cases was negligible, indicating that the steric effect is not significant for the propagation reaction. On the other hand, the activation enthalpy difference, $\Delta H^{\ddagger}_{EMA\text{-}EMA} - \Delta H^{\ddagger}_{EMA\text{-}MMA}$, was approximately three times higher than $\Delta H^{\ddagger}_{MMA\text{-}MMA} - \Delta H^{\ddagger}_{MMA\text{-}EMA}$. These results strongly suggest that more energy is needed for the EMA radical with MMA than for the MMA radical with EMA, and hence, the resulting copolymer does not exhibit a perfectly random sequence, further explaining the compositional variation at high conversion. The dyad fractions extracted from the reactivity ratios provide a tool for predicting the glass transition behaviors of the copolymers; the Johnston and Barton models, which make use of the dyad information, but not the Fox and Gibbs-DiMarzio models, described the composition dependence of $T_g$. Finally, the chain extension of the random copolymers with styrene via RAFT polymerization confirmed that the chain ends can still be activated, highlighting the effectiveness of the copolymerization by Cu(0)-mediated RDRP to achieve complex copolymer architectures. These findings should provide a deeper understanding of the fundamental aspects and a tool to gain insight into the sequence of copolymers synthesized via RDRP, which can ultimately be correlated to a variety of physical and chemical properties.

**Acknowledgements** We gratefully acknowledge the support from the National Research Foundation of Korea (NRF) (Grant No. 2017M2A2A6A01018631).

**Competing interests** The authors declare no competing interests.

## References

1. Mapas JKD, Thomay T, Cartwright AN, Ilavsky J, Rzayev J. Ultrahigh molecular weight linear block copolymers: rapid access by reversible-deactivation radical polymerization and

self-assembly into large domain nanostructures. Macromolecules. 2016;49:3733–8.
2. Braunecker WA, Matyjaszewski K. Controlled/living radical polymerization: features, developments, and perspectives. Prog Polym Sci. 2007;32:93–146.
3. Matyjaszewski K, Xia J. Atom transfer radical polymerization. Chem Rev. 2001;101:2921–90.
4. Treat NJ, Sprafke H, Kramer JW, Clark PG, Barton BE, de Alaniz JR, et al. Metal-Free atom transfer radical polymerization. J Am Chem Soc. 2014;136:16096–101.
5. Percec V, Guliashvili T, Ladislaw JS, Wistrand A, Stjerndahl A, Sienkowska MJ, et al. Ultrafast synthesis of ultrahigh molar mass polymers by metal-catalyzed living radical polymerization of acrylates, methacrylates, and vinyl chloride mediated by SET at 25 °C. J Am Chem Soc. 2006;128:14156–65.
6. Anastasaki A, Nikolaoua V, Haddleton DM. Cu(0)-mediated living radical polymerization: recent highlights and applications; a perspective. Polym Chem. 2016;7:1002–26.
7. Zhang Z, Wang W, Xia H, Zhu J, Zhang W, Zhu X. Single-electron transfer living radical polymerization (SET-LRP) of methyl methacrylate (MMA) with a typical RAFT agent as an initiator. Macromolecules. 2009;42:7360–6.
8. Anastasaki A, Nikolaou V, Nurumbetov G, Wilson P, Kempe K, Quinn JF, et al. Cu(0)-mediated living radical polymerization: a versatile tool for materials synthesis. Chem Rev. 2016;116:835–77.
9. Lligadas G, Percec V. Ultrafast SET-LRP of methyl acrylate at 25 $^{o}$C in alcohols. J Polym Sci A. 2008;46:2745–54.
10. Barbey R, Lavanant L, Paripovic D, Schüwer N, Sugnaux C, Tugulu S, et al. Polymer brushes via surface-initiated controlled radical polymerization: synthesis, characterization, properties, and applications. Chem Rev. 2009;109:5437–527.
11. Patten TE, Matyjaszewski K. Atom transfer radical polymerization and the synthesis of polymeric materials. Adv Mater. 1999;10:901–15.
12. Chu DSH, Schellinger JG, Shi J, Convertine AJ, Stayton PS, Pun SH. Application of living free radical polymerization for nucleic acid delivery. Acc Chem Res. 2012;45:1089–99.
13. Grishin DF, Grishin ID. Controlled radical polymerization: prospects for application for industrial synthesis of polymers (review). Russ J Appl Chem. 2011;84:2021–8.
14. Chen M, Zhong M, Johnson JA. Light-controlled radical polymerization: mechanisms, methods, and applications. Chem Rev. 2016;116:10167–211.
15. Zetterlund PB, Thickett SC, Perrier S, Bourgeat-Lami E, Lansalot M. Controlled/living radical polymerization in dispersed systems: an update. Chem Rev. 2015;115:9745–9800.
16. Li X, Mastan E, Wang W-J, Li B-G, Zhu S. Progress in reactor engineering of controlled radical polymerization: a comprehensive review. React Chem Eng. 2016;1:23–59.
17. Bates FS. Polymer-polymer phase behavior. Science. 1991;251:898–905.
18. Choi JW, Kim M, Safron NS, Arnold MS, Gopalan P. Transfer of pre-assembled block copolymer thin film to nanopattern unconventional substrates. ACS Appl Mater Interfaces. 2014;6:9442–8.
19. Han E, Kim M, Gopalan P. Chemical patterns from surface grafted resists for directed assembly of block copolymers. ACS Nano. 2012;6:1823–9.
20. Mansky P, Liu Y, Huang E, Russell TP, Hawker C. Controlling polymer-surface interactions with random copolymer brushes. Science. 1997;275:1458–60.
21. Han E, Stuen KO, Leolukman M, Liu C-C, Nealey PF, Gopalan P. Perpendicular orientation of domains in cylinder-forming block copolymer thick films by controlled interfacial interactions. Macromolecules. 2009;42:4896–901.
22. Han E, Gopalan P. Cross-linked random copolymer mats as ultrathin nonpreferential layers for block copolymer self-assembly. Langmuir. 2010;26:1311–5.
23. Schmitt SK, Trebatoski DJ, Krutty JD, Xie AW, Rollins B, Murphy WL, et al. Peptide conjugation to a polymer coating via native chemical ligation of azlactones for cell culture. Biomacromolecules. 2016;17:1040–7.
24. Discekici EH, Pester CW, Treat NJ, Lawrence J, Mattson KM, Narupai B, et al. Simple benchtop approach to polymer brush nanostructures using visible-light-mediated metal-free atom transfer radical polymerization. ACS Macro Lett. 2016;5:258–62.
25. Page ZA, Narupai B, Pester CW, Zerdan RB, Sokolov A, Laitar DS, et al. Novel strategy for photopatterning emissive polymer brushes for organic light emitting diode applications. ACS Cent Sci. 2017;3:654–61.
26. Sweat DP, Kim M, Yu X, Schmitt SK, Han E, Choi JW, et al. Functional layer for block copolymer self-assembly and the growth of nanopatterned polymer brushes. Langmuir. 2013;29:12858–65.
27. Cordero R, Jawaid A, Hsiao M-S, Lequeux Z, Vaia RA, Ober CK. Mini monomer encapsulated emulsion polymerization of PMMA using aqueous ARGET ATRP. ACS Macro Lett. 2018;7:459–63.
28. Letchford K, Burt H. A review of the formation and classification of amphiphilic block copolymer nanoparticulate structures: micelles, nanospheres, nanocapsules and polymersomes. Eur J Pharm Biopharm. 2007;65:259–69.
29. Jones M-C, Leroux J-C. Polymeric micelles – a new generation of colloidal drug carriers. Eur J Pharm Biopharm. 1999;48:101–11.
30. Kataoka K, Harada A, Nagasaki Y. Block copolymer micelles for drug delivery: design, characterization and biological significance. Adv Drug Deliv Rev. 2001;47:113–31.
31. Moughton AO, Hillmyer MA, Lodge TP. Multicompartment block polymer micelles. Macromolecules. 2012;45:2–19.
32. Fernández-García M, Torrado MF, Martínez G, Sánchez-Chaves M, Madruga EL. Free radical copolymerization of 2-hydroxyethyl methacrylate with butyl methacrylate: determination of monomer reactivity ratios and glass transition temperatures. Polymer. 2000;41:8001–8.
33. Tobita H, Hamielec AE. Kinetics of free-radical copolymerization: the pseudo-kinetic rate constant method. Polymer. 1991;32:2641–7.
34. Davis TP, O'Driscoll KF, Piton MC, Winnik MA. Determination of propagation rate constants for the copolymerization of methymethacrylate and styrene using a pulsed laser technique. Polym Lett. 1989;27:181–5.
35. Buback M, Kurz CH. Free-radical propagation rate coefficients for cyclohexyl methacrylate, glycidyl methacrylate and 2-hydroxyethyl methacrylate homopolymerizations. Macromol Chem Phys. 1998;199:2301–10.
36. Beuermann S, Buback M, Hesse P, Lacík I. Free-radical propagation rate coefficient of nonionized methacrylic acid in aqueous solution from low monomer concentrations to bulk polymerization. Macromolecules. 2006;39:184–93.
37. Haddleton DM, Crossman MC, Hunt KH, Topping C, Waterson C, Suddaby KG. Identifying the nature of the active species in the polymerization of methacrylates: inhibition of methyl methacrylate homopolymerizations and reactivity ratios for copolymerization of methyl methacrylate/*n*-butyl methacrylate in classical anionic, alkyllithium/trialkylaluminum-initiated, group transfer polymerization, atom transfer radical polymerization, catalytic chain transfer, and classical free radical polymerization. Macromolecules. 1997;30:3992–8.
38. Ritz P, Látalová P, Kříž J, Genzer J, Vlček P. Statistical copolymers of 2-(trimethylsilyloxy)ethyl methacrylate and methyl methacrylate synthesized by ATRP. J Polym Sci A. 2008;46:1919–23.

39. Rajendrakumar K, Dhamodharan R. Ambient temperature atom transfer radical copolymerization of tetrahydrofurfuryl methacrylate and methyl methacrylate: reactivity ratio determination. Eur Polym J. 2009;45:2685–94.
40. Roka N, Kokkorogianni O, Pitsikalis M. Statistical copolymers of n-vinylpyrrolidone and 2-(dimethylamino)ethylmethacrylate via RAFT: monomer reactivity ratios, thermal properties, and kinetics of thermal decomposition. J Polym Sci A. 2017;55:3776–87.
41. Holmberg AL, Karavoliasa MG, Epps III TH. RAFT polymerization and associated reactivity ratios of methacrylate-functionalized mixed bio-oil constituents. Polym Chem. 2015;6:5728–39.
42. Gao J, Zhang Z, Zhou N, Cheng Z, Zhu J, Zhu X. Copper(0)-mediated living radical copolymerization of styrene and methyl methacrylate at ambient temperature. Macromolecules. 2011;44:3227–32.
43. Uragami T, Yamada H, Miyata T. Removal of dilute volatile organic compounds in water through graft copolymer membranes consisting of poly(alkylmethacrylate) and poly(dimethylsiloxane) by pervaporation and their membrane morphology. J Memb Sci. 2001;187:255–69.
44. Qi D, Bai F, Yang X, Huang W. Synthesis of core-shell polymer microspheres by two-stage distillation–precipitation polymerization. Eur Polym J. 2005;41:2320–8.
45. Yang J, Hu J, Wang C, Qin Y, Guo Z. Fabrication and characterization of soluble multi-walled carbon nanotubes reinforced P (MMA-*co*-EMA) composites. Macromol Mater Eng. 2004;289:828–32.
46. Matyjaszewski K, Davis KA. Statistical copolymers. Adv Polym Sci. 2002;159:14–29.
47. Liu G, Zhang L, Wang Y, Zhao P. Studies on binary copolymerization and glass transition temperatures of methyl methacrylate with ethyl methacrylate and n-butyl methacrylate. J Appl Ploym. 2009;114:3939–44.
48. Fischer H. The persistent radical effect in controlled radical polymerizations. J Polym Sci A. 1999;37:1885–901.
49. Barner-Kowollik C, Buback M, Charleux B, Coote ML, Drache M, Fukuda T, et al. Mechnism and kinetics of dithiobenzoate-mediated RAFT polymerization. I. The current situation. J Polym Sci A. 2006;44:5809–31.
50. Perrier S, Barner-Kowollik C, Quinn JF, Vana P, Davis TP. Origin of inhibition effects in the reversible addition fragmentation chain transfer (RAFT) polymerization of methyl acrylate. Macrmolecules. 2002;35:8300–6.
51. Mayo FR, Lewis FM, Copolymerization. I. A basis for comparing the behavior of monomers in copolymerization; the copolymerization of styrene and methyl methacrylate. J Am Chem Soc. 1944;66:1594–601.
52. Fineman M, Ross SD. Linear method for determining monomer reactivity ratios in copolymerization. J Polym Sci A. 1950;5:259–65.
53. Kelen T, Tüdös F, Turcsányi B. Confidence intervals for copolymerization reactivity ratios determined by the Kelen-Tüdös method. Polym Bull. 1980;2:71–76.
54. Manders BG, Smulders W, Aerdts AM, van Herk AM. Determination of reactivity ratios for the system methyl methacrylate-*n*-butyl methacrylate. Macromolecules. 1997;30:322–3.
55. Grassie N, Torrance BJD, Fortune JD, Gemmell JD. Reactivity ratios for the copolymerization of acrylates and methacrylates by nuclear magnetic resonance spectroscopy. Polymer. 1965;6:653–8.
56. Lewis FM, Walling C, Cummings W, Briggs ER, Mayo FR. Copolymerization. IV. Effets of temperature and solvents on monomer reactivity ratio. J Am Chem Soc. 1948;70:1519–23.
57. Barson CA, Rizvi MS. The temperature dependence of the monomer reactivity ratio in the copolymerization of styrene and cinnamic acid. Eur Polym J. 1970;6:241–6.
58. Chûjô R, Ubara H, Nishioka A. Determination of monomer reactivity ratios in copolymerization from a single sample and its application to the acrylonitrile–methyl methacrylate system. Polym J. 1972;3:670–4.
59. Fox Jr TG, Flory PJ. Second-order transition temperatures and related properties of polystyrene. I. Influence of molecular weight. J Appl Phys. 1950;21:581–91.
60. Dimarzio EA, Gibbs JH. Molecular interpretation of glass temperature depression by plasticizers. J Polym Sci A. 1963;1:1417–28.
61. Johnston NW. Sequence distribution-glass transition effects. J Macromol Sci C. 1976;14:215–50.
62. Barton JM. Relation of glass transition temperature to molecular structure of addition copolymers. J Polym Sci Part C: Polym Symp. 1970;30:573–97.
63. Hiemenz PC, Lodge TP. Polymer Chemistry, 2nd edn., CRC Press; (Boca Raton, FL USA. 2007).